nature astronomy

Article

https://doi.org/10.1038/s41550-023-01902-4

Enhanced star formation through the high-temperature formation of H_2 on carbonaceous dust grains

Received: 29 July 2022

Accepted: 25 January 2023

Published online: 02 March 2023

Check for updates

Francesco Grieco[1,2], Patrice Theulé[3], Ilse De Looze[2] & François Dulieu[1]

The microphysics of molecular hydrogen formation has an influence on galactic-scale star-formation rates over cosmic time. H_2 is the cooling agent needed to initiate the cloud collapse regulating the star-formation efficiency. H_2 formation is inefficient in the gas phase under typical interstellar conditions, requiring dust grain surfaces to act as catalysts. Small carbonaceous grains with sizes from roughly 4 to 100–200 Å, including polycyclic aromatic hydrocarbons (PAHs), have been shown to increase the H_2 formation rates due to their large surface-to-volume ratios. H_2 formation rates on PAHs were previously thought to reduce above temperatures of 50 K and H atom recombination was believed to be highly efficient only below 20 K. Until now, both laboratory experiments and theoretical modelling have suggested that H_2 cannot form on grains with temperatures above 100 K. Here we report evidence, through direct laboratory measurements, of the highly efficient formation of H_2 at temperatures up to 250 K on carbonaceous surfaces mimicking interstellar dust. By pushing their formation towards warmer temperatures, the H_2 molecules could start contributing substantially to the cooling of warmer gas (temperatures of roughly 50–250 K). This will have a marked impact on our understanding of H_2 formation in nearby galaxies and its efficiency in high-redshift galaxies where the Cosmic Microwave Background already pushes dust temperatures to more than 20 K.

Molecular hydrogen H_2 is the smallest, simplest but most abundant of the molecules in the Universe, its abundance (1) shapes the molecular phases of the interstellar medium (ISM) where stars are formed because its self-shielding from the interstellar radiation[1] controls the extent of the photodissociation regions H_2 (ref. [2]), and (2) regulates the star-formation efficiency through the effect of H_2 and the subsequent molecules formed, cooling lines on the ISM cooling function for gas temperature $T \leq 10^4$ K (refs. [3,4]). Molecular hydrogen has three major routes of formation: (1) the H^+ route ($H + H^+ \rightarrow H_2^+ + h\nu$, $H_2^+ + H \rightarrow H_2 + H^+$), which dominates for redshifts z of roughly 400, (2) the H^- route ($H + e^- \rightarrow H^- + h\nu$, $H^- + H \rightarrow H_2 + e^-$), which dominates for a z of roughly 100 and (3) the grain surface catalytic route ($H + H$ + surface $\rightarrow H_2$ + surface), which dominates in the local Universe ($z = 0$). The two gas phase routes dominate in the primordial gas of the Early Universe and, although inefficient, they play a main role in the formation of the first stars (population III stars).

The dominant H_2 formation route depends on the presence of dust grains, and hence on the metallicity and the dust temperature. H_2 formation on dust grains can also dominate at redshift 6–7, after the formation of the first stars and the enrichment of the ISM with metals and dust grains[5,6]. Our present study focuses on this third and major route. The process of H_2 formation on interstellar grains can be

[1]CY Cergy Paris University, Observatory of Paris, PSL University, Sorbonne University, CNRS, LERMA, Cergy, France. [2]Department of Physics and Astronomy, University of Ghent, Ghent, Belgium. [3]Aix Marseille University, CNRS, CNES, LAM, Marseille, France. e-mail: francois.dulieu@cyu.fr

https://doi.org/10.1038/s41550-023-01902-4

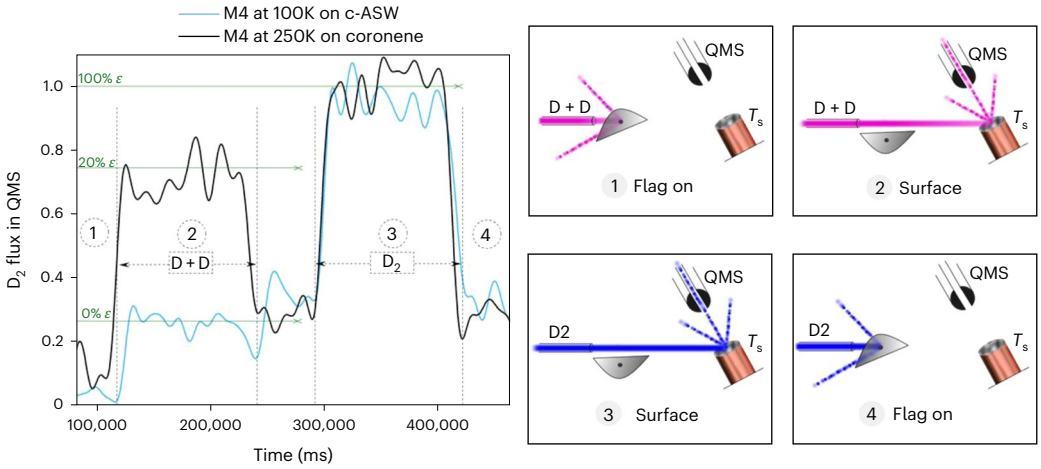

Fig. 1 | Experimental setup and protocol. Comparison between M4 (D_2, m/z 4) signals by using coronene (black line, T_s = 250 K) and c-ASW (light blue line, T_s = 100 K) as surfaces (left); four schematic configurations of FORMOLISM including position and role of the flag, position of the QMS associated to the four divisions of the signal shown on the left (right). The green lines show the values of the recombination efficiencies (ε).

summarized in three steps. The first consists of the sticking of atoms from the gas phase on the grain surfaces, the second relates to the diffusion and reactivity of the atoms on the surface and the third to the return of the molecule to the gas phase. The most critical step is the second one, as, depending on the temperature of the grain, the atoms already adsorbed can desorb before a new atom arrives, making the recombination impossible. This is why on a water ice surface, for example, as the binding energy of physisorbed H is low (residence time of H short for rising temperature), the recombination efficiency decreases abruptly beyond 12–15 K (ref. [7]). The same has been observed for silicate surfaces[8]. The range is wider for graphite or amorphous carbon surfaces[9] but, overall, if the atoms cannot chemisorb (that is, make a covalent bond with the surface), the formation efficiency can no longer be important beyond 20 K, due to the fast desorption of H. On an aliphatic carbon surface, HD recombination has been reported at higher temperatures but with low cross sections[10]. If the atoms can chemisorb, then Cazaux et al.[11] estimated that H_2 formation ought to reduce above 50 K and slowly decrease to zero at 150 K. Many studies on H sticking, diffusion and recombination on different surfaces have been performed and are collected in the review article by Wakelam et al.[12]. However, none has performed a direct measurement of the recombination efficiency at temperatures above 20 K.

Astrophysical importance

Dust grains at high redshift are probably partly in the form of very small graphitic grains (PAHs). In fact, both in the nearby and high-redshift Universe, one can see evidence for the PAH mass fraction correlates with metallicity[13,14] due to harder and more intense radiation fields in low-metallicity galaxies. Given the high dust masses in several high-redshift galaxies, rather high metallicities are expected. Indeed, both observations and models suggest that the metallicity can already be around 20% of the solar value[15,16], which would still allow for sufficient PAHs to be present in these high-z galaxies. Recent ALMA (Atacama large millimetre/submillimetre array) observations have demonstrated the presence of large quantities of dust already at redshifts of roughly z = 6–9 (refs. [17–19]; Spilker, J. S. et al., unpublished manuscript); it is likely that H_2 formation on dust grains is already the dominant mechanism in those galaxies. Theoretical models predict dust temperatures in high-redshift giant molecular clouds above 60 K (ref. [20]), while estimates from observational studies range between 40 and 80 K (refs. [21–23]). The fact that star formation is efficient in these galaxies suggests that H_2 formation must also be efficient at those temperatures to enable high levels of star-formation activity. The experimental results reported in this paper have the potential to revolutionize our understanding of the formation of the first generations of stars at high redshift. The high H_2 formation rate estimated from the observation of photodissociation region (PDR) has been proposed to be due to the catalytic effect of PAH[24] and its propensity to do chemisorption has been calculated[25]. There are several studies in the literature highlighting that the presence of small carbonaceous grains, with large surface-to-volume ratios in comparison to large grains, increases the H_2 formation rates[24,26]. Direct experimental results supporting the hypothesis of PAHs as active catalysts for H_2 formation under interstellar conditions have so far been lacking. This study provides a breakthrough in experimental insights and will finally enable an estimation of the contribution of PAHs to interstellar H_2 formation at higher temperatures until now not considered.

Experimental protocol and results

Figure 1 shows the protocol we use to measure the recombination efficiency of D into D_2, for a given surface and temperature. The experiments are carried out with the FORMOLISM (formation of molecules in the interstellar medium) setup: an ultra-high vacuum (UHV) chamber hosting a copper sample holder, connected to a cryostat, in which the coronene film surface is deposited. The beamline containing D_2 aims towards the surface where the temperature-dependent results reported in this paper are measured. The detection is made by a quadrupole mass spectrometer (QMS). More details about the specifics of the setup used can be found in the Methods section.

For the recombination efficiency experiments, the QMS is placed in front of the surface and mostly measures what is coming off the surface (plus some unavoidable background contribution from the wall of the chamber). The beam, dissociated (1, 2) or not (3, 4), can be intercepted by the flag (1, 4) (Fig. 1). In this way, we can subtract the contribution of the chamber. The black curve on the left panel is the measurement of the M4 (m/z = 4 corresponding to D_2) using a coronene film held at 250 K as a surface, whereas the blue curve is for an amorphous compact solid water ice film (c-ASW) of 30 layers of thickness deposited on the sample holder at 100 K. The ice film has been deposited to validate our protocol and to prove the difference in results with respect to when coronene is used as a surface. For the blue curve, we observe no increase of the M4 when the dissociated beam is aimed at the surface. The increase between steps 1 and 2 is only due to the undissociated part of the beam. On the contrary, we observe a clear increase of the signal when the coronene film is used (black curve). This is direct evidence that, in the case of coronene films, D_2 molecules are formed and readily desorb to be detected by the QMS. In the case of

https://doi.org/10.1038/s41550-023-01902-4

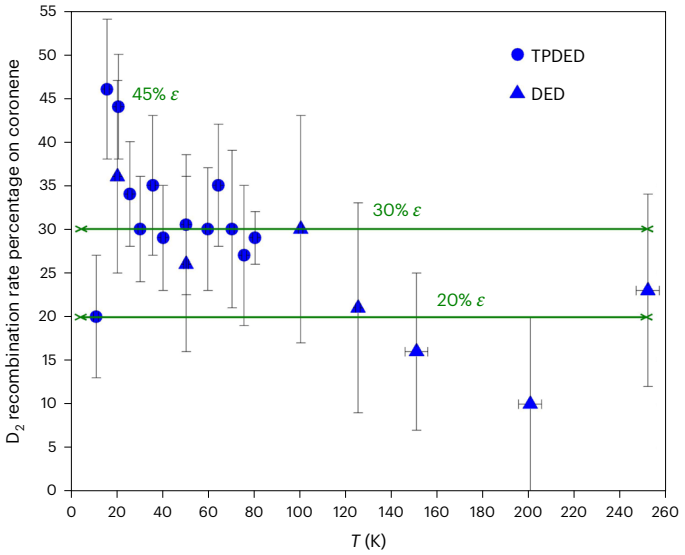

Fig. 2 | Recombination efficiency (ε) of D_2 on coronene. Temperature-dependent percentage recombination efficiency (ε) of D_2 on coronene. Circles denote temperature-programmed DED experiments; triangles show DED isothermal experiments. Data are presented as mean values ± s.e.m. (1 − sigma error), in which the error bars are derived from each component of the equation of ε. Those components are each the average of the signal recorded at a specific temperature for that setup configuration (flag on (BKG) or off, plasma on or off), each providing a different sample size (n number) depending on its detection time.

water ice, as expected, the contribution of D_2 formation is measured as negligible, which demonstrates the robustness of the protocol. From this graph, and accounting for the dissociation efficiency, we can calculate the efficiency of D + D recombination mediated by the surface at a given temperature. As the total signal of M4 detected when the plasma is on is equal to the background signal plus the undissociated part of the beam and the signal from recombination, the efficiency (ε) is therefore expressed as follows:

$$\varepsilon = (\mathrm{M4}_{\mathrm{plasma\ on}} - \mathrm{BKG}_{\mathrm{plasma\ on}}) - (\mathrm{M4}_{\mathrm{plasma\ off}} - \mathrm{BKG}_{\mathrm{plasma\ off}}) \times (1 - \tau)$$

where $\mathrm{M4}_{\mathrm{plasma\ on}} - \mathrm{BKG}_{\mathrm{plasma\ on}}$ is the total signal detected with the QMS when the plasma is ON after background (BKG) subtraction; $(\mathrm{M4}_{\mathrm{plasma\ off}} - \mathrm{BKG}_{\mathrm{plasma\ off}}) \times (1 - \tau)$ is the part of the signal coming from the undissociated molecules and where τ represents the dissociation efficiency (%) measured before and after each experiment (see the Supplementary Information for the details of its calculation). ε is normalized to the signal of $m/z = 4$ detected when the plasma was off subtracted from its background ($\mathrm{M4}_{\mathrm{plasma\ off}} - \mathrm{BKG}_{\mathrm{plasma\ off}}$). ε corresponds to the probability of an atom impinging the surface to recombine and be detected as a molecule, it includes all steps of accretion, diffusion and reaction. The definition of recombination efficiency can therefore differ depending on the inclusion of those steps. In Cazaux and Spaans[5], the quantity displayed does not include the accretion (that is, sticking) phase.

Figure 2 displays the variation of ε with the surface temperature. The points at temperature above 100 K have been performed at a fixed temperature, whereas the points below have been measured on the fly, using the temperature-programmed during exposure desorption (DED) technique with a 1 K min^{-1} ramp[27]. The error bars have been estimated by adding all sources of uncertainties, including the most extreme fluctuations of the dissociation efficiency that makes the biggest contribution in the uncertainty. We observe a plateau above 100 K, at around 20%, a higher value at around 30% between 30 and 80 K, two extreme values around 20 K and a sharp decrease at 10 K. The reduction of efficiency at 10 K is due to the presence of adsorbed molecules. The presence of pre-adsorbed molecules reduces the direct contribution of formed molecules, as similarly observed on water ice films[28]. The overall efficiency of the recombination depends on different competing mechanisms. The sticking or accretion is not supposed to be very dependent on the surface temperature in this range[29] and it should be around 0.5, which is in line with our upper value of ε. This is due to the corrugated nature of our coronene, contrarily to when graphite is used as substrate, where coronene forms an uniform and flat film. The desorption of atoms is increasing exponentially with the temperature, and should become a dominant loss channel. For a typical binding energy of 45 meV, the residence time is hundred picoseconds at 60 K, therefore, the only chance for an atom to recombine is to be incorporated in a chemisorption site. Fortunately, C–H termination of PAH can procure such chemisorption sites. This was first proposed and calculated by Rauls and Hornekaer[25], and the inclusion of D atoms to coronene has been experimentally demonstrated later[30]. Mennella[10] has also shown that the aliphatic group could also have a similar catalytic role, despite its lower cross section. The plateau at around 20% for temperatures greater than 80–100 K is therefore the probability of a D atom to react with an extra D atom already chemisorbed on the surface or to find a default site in the coronene film. We note here that there should be a barrier for the first hydrogenation, but that has no real importance in steady state conditions such as in our experimental protocol. The results were found constant after an exposition of a few 10^{15} atoms per cm^2, which correspond to a film of coronene just slightly superhydrogenated[30]. When the surface temperature is reduced, the D residence time on the surface increases exponentially, and the physisorption–chemisorption transfer is probably favoured. The maximum is obtained for a surface slightly higher than 20 K where the surface is still free of D_2 molecules that could have adsorbed. Below this temperature, D_2 molecule coverage increases and may prevent D atoms from accessing reactive sites/partners, simply by reducing their accretion rate on the surface. This must be studied in better detail in forthcoming experiments. Considering that small carbonaceous grains make a dominant contribution to the total grain surface and have numerous chemically bonded hydrogen atoms, we demonstrate that they play a key role in H_2 formation by chemisorption. Our study shows that the H_2 formation pathway on surfaces can be much more efficient than previously estimated, and over an extended range of temperatures.

Astrophysical implications

As soon as carbonaceous dust appears, the cooling capacity of the ISM increases sharply, and thus its condensation in pre-stellar cores. Our work on molecular hydrogen surface formation involving chemisorption on carbon surface at temperatures around 100–200 K is of prime importance in astrophysics. It will change the location of the H/H_2 photodissociation front and the respective size of HII regions, PDR and molecular regions in a classical PDR picture[2]. Our results may furthermore explain the under-prediction of observed H_2 column densities by models[31] and the shift of the H/H_2 transition closer to the ionization front in resolved PDRs[32]. Additionally, our work brings one possibility to solve the contradiction between the possible discovery of James Webb telescope ultra-high-redshift galaxies on one hand[33], and on the other, the redshift limit above which stars could not have formed, obtained by crossing the efficiency of H_2 formation against dust temperature and the dust temperature dependence against the redshift[21,34–36] with a minimum temperature ultimately defined by the CMB. The warmer CMB of high-redshift galaxies is observed in the (sub-)millimetre dust continuum and the line emission as it provides an additional source of heating[37,38].

Correctly accounting for molecular hydrogen formation over cosmic times is a key ingredient to interpreting the James Webb telescope observations not only in the local Universe, for the H_2 lines in nearby galaxies, but also for atomic and molecular emission lines of high-redshift galaxies in general.

Methods

The experiments were performed on the FORMOLISM experimental setup described in more detail in Congiu et al.[39]. Briefly, the apparatus is composed of an UHV stainless steel chamber with a base pressure of a few 10^{-11} hPa (1 hPa = 1 mbar). The sample holder is made of a 1-cm-diameter copper block, thermally connected to a cold finger of a closed-cycle He cryostat and located in the centre of the main chamber. A few layers of coronene ($C_{24}H_{12}$) are deposited on the sample holder held at 280 K from a movable crucible placed at 3 cm from it. The coronene film is a corrugated surface, probably made of disordered stack or small clusters of coronene, mimicking dust particles with surface defects.

A beam of D atoms is aimed at the surface through a triple stage of differential pumping. A D isotope is used instead of H, because H_2 is the major contaminant of any UHV system and will give a better signal-to-noise ratio. When the beam is aimed at the surface, the overall pressure in the main chamber only rises by 1×10^{-11} hPa, and the partial pressure directly in the beam at the surface is estimated to be roughly 2×10^{-8} hPa. In such conditions, D atoms land on a surface adsorption site roughly every 100 s. The atoms are produced from a plasma discharge, but the D_2 dissociation efficiency is not perfect. The atoms are at a temperature slightly above the room temperature (<350 K) and approach from the surface at an angle of 40°, thus reducing their kinetic energy perpendicular to the surface. The detection tool of this setup is a QMS that can be rotated to be placed in front of the beams or the surface depending on the type of the experiments. In our experimental methodology, there are a few important points to stress before going into their technical details.

To infer the efficiency for the atoms to scan the surface and recombine to form molecules, it is indeed extremely crucial to calculate the amount of them produced by our system when the plasma is switched on (when off, only D_2 reaches the surface) and the level of the background partial pressure present in the chamber. Those determinations will help in assessing the amount of D_2 molecules due to the recombination of the atoms reaching the surface and to exclude any effect coming from a change of the background signal during experiments. Supplementary Fig. 1 shows the protocol followed to estimate the ratio of D_2 and D in a given experiment.

Data availability

Metadata have been created on our laboratory platform to make sure that an online version of each set of data is always available and reachable by each member of the laboratory group, or researchers working on the project. Files are automatically released after 3 years from the uploading date. The data that support the findings of this study are available from the corresponding author upon reasonable request.

References

1. Hartwig, T., Glover, S. C. O., Klessen, R. S., Latif, M. A. & Volonteri, M. How an improved implementation of H_2 self-shielding influences the formation of massive stars and black holes. *Mon. Not. R. Astron. Soc.* **452**, 1233–1244 (2015).
2. Tielens, A. G. G. M. & Hollenbach, D. Photodissociation regions. I—Basic model. II—A model for the Orion photodissociation region. *Astrophys. J.* **291**, 722 (1985).
3. Glover, S. C. O. & Clark, P. C. Molecular cooling in the diffuse interstellar medium. *Mon. Not. R. Astron. Soc.* **437**, 9–20 (2014).
4. Bigiel, F. et al. The star formation law in nearby galaxies on sub-kpc scales. *Astron. J.* **136**, 2846 (2008).
5. Cazaux, S. & Spaans, M. Molecular hydrogen formation on dust grains in the high-redshift universe. *Astrophys. J.* **611**, 40–51 (2004).
6. Algera, H. et al. The ALMA REBELS Survey: the dust-obscured cosmic star formation rate density at redshift 7. Preprint at *arXiv* https://doi.org/10.48550/arXiv.2208.08243 (2022).
7. Amiaud, L., Dulieu, F., Fillion, J.-H., Momeni, A. & Lemaire, J. L. Interaction of atomic and molecular deuterium with a nonporous amorphous water ice surface between 8 and 30 K. *J. Chem. Phys.* **127**, 144709 (2007).
8. Pirronello, V., Biham, O., Liu, C., Shen, L. & Vidali, G. Efficiency of molecular hydrogen formation on silicates. *Astrophys. J.* **483**, L131–L134 (1997).
9. Vidali, G. H_2 formation on interstellar grains. *Chem. Rev.* **113**, 8762–8782 (2013).
10. Mennella, V. HD formation by abstraction of H/D chemisorbed in carbon grains with D/H atoms under simulated interstellar conditions. *Astrophys. J.* **684**, L25 (2008).
11. Cazaux, S. et al. The sequence to hydrogenate coronene cations: a journey guided by magic numbers. *Sci. Rep.* **6**, 19835 (2016).
12. Wakelam, V. et al. H_2 formation on interstellar dust grains: the viewpoints of theory, experiments, models and observations. *Mol. Astrophys.* **9**, 1–36 (2017).
13. Galliano, F. et al. A nearby galaxy perspective on dust evolution: scaling relations and constraints on the dust build-up in galaxies with the DustPedia and DGS samples. *Astron. Astrophys.* **649**, A18 (2021).
14. Shivaei, I. et al. The MOSDEF survey: metallicity dependence of PAH emission at high redshift and implications for 24 μm inferred IR luminosities and star formation rates at $z \sim 2$. *Astrophys. J.* **837**, 157 (2017).
15. Jones, T. et al. The mass-metallicity relation at $z \simeq 8$: direct-method metallicity constraints and near-future prospects. *Astrophys. J.* **903**, 150 (2020).
16. Dayal, P. et al. The ALMA REBELS survey: the dust content of z7 Lyman break galaxies. *Mon. Not. R. Astron. Soc.* **512**, 989–1002 (2022).
17. Watson, D. et al. A dusty, normal galaxy in the epoch of reionization. *Nature* **519**, 327–330 (2015).
18. Pozzi, F. et al. The ALPINE-ALMA [CII] survey: dust mass budget in the early Universe. *Astron. Astrophys.* **653**, A84 (2021).
19. Riechers, D. A. et al. Polycyclic aromatic hydrocarbon and mid-infrared continuum emission in a $z > 4$ submillimeter galaxy. *Astrophys. J.* **786**, 31 (2014).
20. Sommovigo, L. et al. Warm dust in high-z galaxies: origin and implications. *Mon. Not. R. Astron. Soc.* **497**, 956–968 (2020).
21. Sommovigo, L. et al. The ALMA REBELS survey: cosmic dust temperature evolution out to z 7. *Mon. Not. R. Astron. Soc.* **513**, 3122–3135 (2022).
22. Faisst, A. L. et al. ALMA characterizes the dust temperature of $z \sim 5.5$ star-forming galaxies. *Mon. Not. R. Astron. Soc.* **498**, 4192–4204 (2020).
23. Bakx, T. J. L. C. et al. ALMA uncovers the [C II] emission and warm dust continuum in a $z = 8.31$ Lyman break galaxy. *Mon. Not. R. Astron. Soc.* **493**, 4294–4307 (2020).
24. Habart, E., Boulanger, F., Verstraete, L., Walmsley, C. M. & Pineau des Forêts, G. Some empirical estimates of the H_2 formation rate in photon-dominated regions. *Astron. Astrophys.* **414**, 531–544 (2004).
25. Rauls, E. & Hornekær, L. Catalyzed routes to molecular hydrogen formation and hydrogen addition reactions on neutral polycyclic aromatic hydrocarbons under interstellar conditions. *Astrophys. J.* **679**, 531–536 (2008).
26. Lipshtat, A. & Biham, O. The effect of grain size distribution on H_2 formation rate in the interstellar medium. *Mon. Not. R. Astron. Soc.* **362**, 666–670 (2005).
27. Minissale, M., Dulieu, F., Cazaux, S. & Hocuk, S. Dust as interstellar catalyst: I. Quantifying the chemical desorption process. *Astron. Astrophys.* **585**, A24 (2016).

28. Congiu, E., Matar, E., Kristensen, L. E., Dulieu, F. & Lemaire, J. L. Laboratory evidence for the non-detection of excited nascent H_2 in dark clouds. *Mon. Not. R. Astron. Soc. Lett.* **397**, L96–L100 (2009).
29. Cazaux, S., Morisset, S., Spaans, M. & Allouche, A. When sticking influences H_2 formation. *Astron. Astrophys.* **535**, A27 (2011).
30. Thrower, J. D. et al. Superhydrogenated PAHs: catalytic formation of H_2. *EAS Publ. Ser.* **46**, 453–460 (2011).
31. Habart, E. et al. Excitation of H_2 in photodissociation regions as seen by. *Spitze. Astron. Astrophys.* **527**, A122 (2011).
32. Habart, E. et al. High angular resolution near-IR view of the Orion Bar revealed by Keck/NIRC2. Preprint at *arXiv* http://arxiv.org/abs/2206.08245 (2022).
33. Finkelstein, S. L. et al. A long time ago in a galaxy far, far away: a candidate $z\sim12$ galaxy in early JWST CEERS imaging. Preprint at *arXiv* https://doi.org/10.48550/arXiv.2207.12474 (2022).
34. Bakx, T. J. L. C. et al. Accurate dust temperature determination in a $z=7.13$ galaxy. *Mon. Not. R. Astron. Soc. Lett.* **508**, L58–L63 (2021).
35. Liang, L. et al. On the dust temperatures of high-redshift galaxies. *Mon. Not. R. Astron. Soc.* **489**, 1397–1422 (2019).
36. Viero, M. P., Sun, G., Chung, D. T., Moncelsi, L. & Condon, S. S. The early Universe was dust-rich and extremely hot. *Mon. Not. R. Astron. Soc. Lett.* **516**, L30–L34 (2022).
37. Cunha, Eda et al. On the effect of the Cosmic Microwave Background in high-redshift (sub-)millimeter observations. *Astrophys. J.* **766**, 13 (2013).
38. Lagache, G., Cousin, M. & Chatzikos, M. The [CII] 158 μm line emission in high-redshift galaxies. *Astro Astrophys.* **609**, A130 (2018).
39. Congiu, E. et al. Efficient surface formation route of interstellar hydroxylamine through NO hydrogenation. I. The submonolayer regime on interstellar relevant substrates. *J. Chem. Phys.* **137**, 054713 (2012).

Acknowledgements

This work has been funded by the European Research Council for the Starting Grant 'DustOrigin', held by I.D.L., University of Ghent, grant agreement ID no. 851622. It was supported by the Agence Nationale de la Recherche (ANR) SIRC project (grant no. ANR-SPV202448 2020-2024). This work was supported by the Programme National 'Physique et Chimie du Milieu Interstellaire' by the Programme National Cosmology et Galaxies of CNRS/INSU with INC/INP and IN2P3, cofunded by CEA and CNES, and by the DIM-ACAV+, a funding programme of the Region Ile de France. F.G. and F.D. thank colleagues from LERMA-CYU for their support.

Author contributions

Experiments were carried out by F.G. with the help of F.D. and P.T. Experimental protocols were designed by F.G. and F.D. Data analysis was done by F.G. with the help of F.D. Discussion of the results for their astrophysical importance and implications was carried out by P.T., I.D.L. and F.D. All the authors listed in this paper have contributed to its writing.

Competing interests

The authors declare no competing interests.

Additional information

Supplementary information The online version contains supplementary material available at https://doi.org/10.1038/s41550-023-01902-4.

Correspondence and requests for materials should be addressed to François Dulieu.

Peer review information *Nature Astronomy* thanks Wing-Fai Thi and Liv Hornekær for their contribution to the peer review of this work.